

Application of meta-model based parameter identification of a seismically retrofitted reinforced concrete building

Eunjong Yu*

Department of Architectural Engineering, Hanyang University, 222 Wangsimni-ro, Seongdong-gu, Seoul 04763, Republic of Korea

(Received November 10, 2017, Revised December 19, 2017, Accepted December 23, 2017)

Abstract. FE models for complex or large-scaled structures that need detailed modeling of structural components are usually constructed using commercial analysis softwares. Updating of such FE model by conventional sensitivity-based methods is difficult since repeated computation for perturbed parameters and manual calculations are needed to obtain sensitivity matrix in each iteration. In this study, an FE model updating procedure avoiding such difficulties by using response surface (RS) method and a Pareto-based multiobjective optimization (MOO) was formulated and applied to FE models constructed with a commercial analysis package. The test building is a low-rise reinforced concrete building that has been seismically retrofitted. Dynamic properties of the building were extracted from vibration tests performed before and after the seismic retrofits, respectively. The elastic modulus of concrete and masonry, and spring constants for the expansion joint were updated. Two RS functions representing the errors in the natural frequencies and mode shape, respectively, were obtained and used as the objective functions for MOO. Among the Pareto solutions, the best compromise solution was determined using the TOPSIS (Technique for Order of Preference by Similarity to Ideal Solution) procedure. A similar task was performed for retrofitted building by taking the updating parameters as the stiffness of modified or added members. Obtained parameters of the existing building were reasonably comparable with the current code provisions. However, the stiffness of added concrete shear walls and steel section jacketed members were considerably lower than expectation. Such low values are seemingly because the bond between new and existing concrete was not as good as the monolithically casted members, even though they were connected by the anchoring bars.

Keywords: model updating; response surface method; multi-objective optimization; seismic retrofit; TOPSIS

1. Introduction

FE model updating is a method to modify uncertain parameters so that the responses of the FE model can replicate the actual responses obtained from experiments or measurement. As one of the methods for model updating, sensitivity-based methods combined with various optimization algorithms are widely recognized (Friswell and Mottershead 1995, Teughels *et al.* 2002, Fang *et al.* 2008, Yu *et al.* 2007, Yu and Chung 2012). In sensitivity-based methods, nonlinear objective functions based on the errors between the measured data and the parameterized model are linearized and the unknown parameters are updated iteratively. In each iteration, the sensitivity matrix representing the effects of changes in each parameter on the responses is evaluated numerically. Thus, when FE models are constructed with commercial FE softwares, the results FE analysis for each parameter perturbation should be collected for sensitivity calculation. This procedure is computationally expensive and performing such work manually would be very difficult and annoying. Furthermore, convergence of the solution is not always guaranteed.

Design of experiments (Montgomery 2008) and statistical approximation techniques using meta-modelling such as the response surface (RS) methodology (Myers and Montgomery 2002) can be good strategies to reduce such computational expense and manual operations. The basic idea of the RS method is to construct surrogate functions by approximating the relationship between the input (structural parameters) and the output (response) obtained at systematically located sampling points. The major benefit of the RS method is the significant reduction in computation cost to reach the optimal point since the surrogate functions are used in lieu of the original analyses.

The model updating is necessarily involved with optimization problem. When two or more quantities are to be matched, the traditional approach is to combine their respective objective functions to form a single-objective function using a weighted sum method (Yu *et al.* 2007, Yu and Chung 2012). In this case, the final solution differs depending on which weighting factors are chosen. The weighting factors should be decided based on the relative importance and noise included in each measurement quantity. However, such information is seldom available and difficult to quantify. A Pareto-based multiobjective optimization method (MOO) (Deb *et al.* 2002, Xitzler and Thiele 1999) can be a good alternative approach to circumvent this problem. While the conventional optimization problem using single or combined objective functions seeks for a unique solution, the MOO generates

*Corresponding author, Associate Professor
E-mail: eunjongyu@hanyang.ac.kr

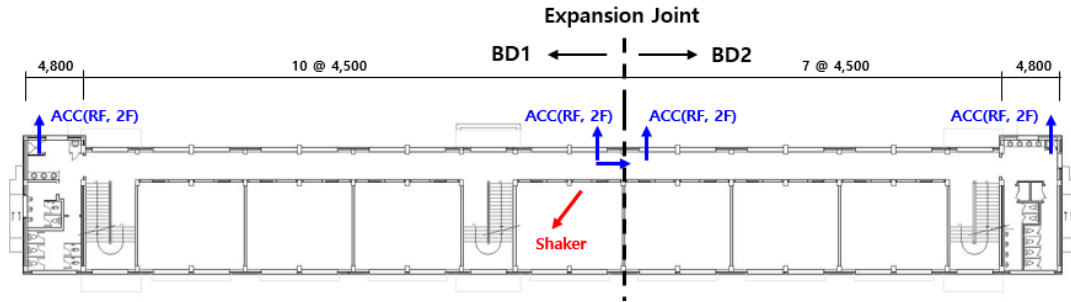


Fig. 1 Location and direction of shaker and accelerometers

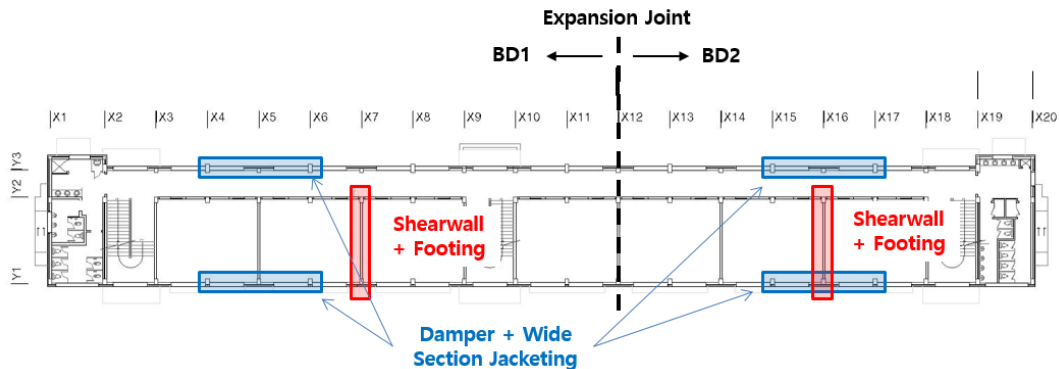


Fig. 2 Seismic retrofit of the building

multiple sets of solutions called as the Pareto solutions.

Generating multiple sets of non-dominant solutions is advantageous since solutions with a permissible violation of objective functions that would not be found by the single-objective function approach can be considered as a candidate for the final solution. A literature survey identified several attempts to apply the RS method for calibrating or updating FE models (Fang and Perera 2009, Fang and Perera 2011, Ren and Chen 2010, Deng and Cai 2009, Shahidi and Pakzad 2013). However, it was found that almost all the reported research regarding the RS method for model updating is based on single or combined objective functions that yield a single optimal solution and the Pareto-based multiobjective optimization approach was seldom studied, despite its flexibility to accommodate trade-offs among multiple objective functions.

Although all of the Pareto solutions are considered equally good in MOO, there is a trade-off between errors in objective functions. Decisions on the final solution among Pareto solutions are made by considering the balance between the errors. Multi-criteria decision-making (MCDM) approaches using posterior evaluation such as the TOPSIS method (Technique for Order of Preference by Similarity to Ideal Solution) (Huang and Yoon 2011, Behzadian *et al.* 2012) can be used to choose the best solution among all Pareto-optimal solutions.

In this study, an FE model updating procedure using the RS method and NSGA-II (Non-dominated Sorting Genetic Algorithm II), a Pareto-based MOO algorithm, was formulated and applied to update analysis models constructed using a commercial FE analysis software. Test building is a low-rise reinforced concrete building that has been seismically retrofitted. Before and after the seismic

retrofit, vibration tests were performed and the dynamic properties of the building were extracted. The concept of TOPSIS was used to determine the final solution among all Pareto-optimal solutions.

2. Vibration testing and system identification of the test building

2.1 Test building

The test structure is a three-story reinforced concrete frame building currently being used as an elementary school. As shown in Fig. 1, the building is separated into two parts by the expansion joint located at line X12. 'BD1' and 'BD2' in the figure denote the left and right parts of the building, respectively.

Vibration testing was carried out using a shaker system with a maximum force capacity of 800 kN, which was installed on the roof. Fig. 1 indicates the location and direction of the shaker and accelerometers. A total of 12 channels of accelerometers were used on the roof and the second floor of BD1 and BD2. The shaker was located at a point away from the center of the building with an inclined direction from the main axis of the building to obtain shaking in all modes as shown in Fig. 1. After testing on BD1 was completed, the shaker was moved to BD2 and an identical test was performed.

This building was seismically retrofitted since seismic performance evaluation of the original building indicated that a large number of the members had deficiencies in resisting the design seismic load. Fig. 2 shows the retrofit measure made in this building. In the transverse direction,

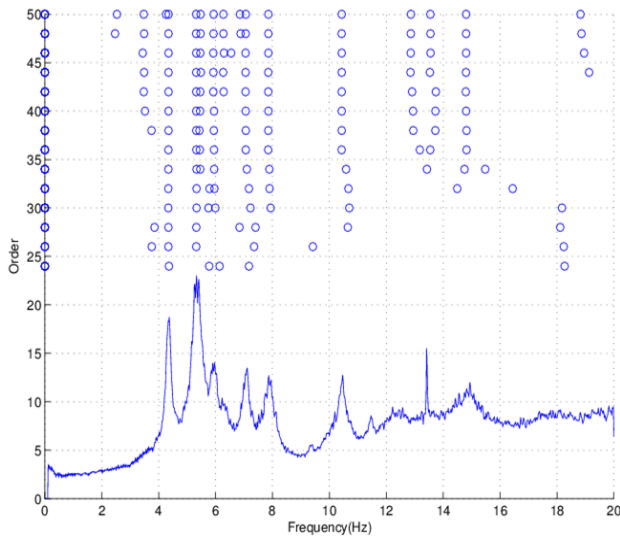


Fig. 3 Stability plot (BD1 shaking, before retrofit)

Table 1 Measured natural frequencies and damping ratios before and after the retrofit

Mode	Natural frequencies (Hz)			Damping ratios (%)		
	Before	After	Ratio	Before	After	Ratio
X-dir in-phase	4.35 (1)	4.22 (1)	97%	2.23	2.69	121%
Y-dir in-phase	5.33 (2)	5.71 (2)	107%	2.47	1.99	81%
X-dir out-of-phase	5.47 (3)	7.18 (5)	131%	0.68	2.15	316%
Y-dir out-of-phase	5.92 (4)	6.22 (3)	105%	1.64	2.33	142%
Torsion in-phase	7.06 (5)	6.76 (4)	96%	1.49	1.76	118%
Torsion out-of-phase	7.85 (6)	8.38 (6)	107%	2.26	2.28	101%

new shear walls with a thickness of 200 mm were casted in place of masonry infills along lines X7 and X16. For retrofit in the longitudinal direction, some of the beams and columns at the exterior were reinforced by steel wide section jacketing and connected with toggle damper systems. In addition, the parquet flooring of the classroom and hallway was replaced by mortar finish for renovation.

2.2 System identification

White noise excitation and subsequent system identification were performed before and after the seismic retrofit. The N4SID (subspace state-space system identification) (Van Overschee and De Moor 1993), one of the time domain methods, was used for system identification. Fig. 3 shows the stability plot representing the variations in identified properties with changes in the order of the state-space model; this was used to distinguish spurious modes from the physical mode.

Fig. 4 shows obtained mode shapes from the first to the sixth mode of pre-retrofit building. It can be seen that the motion of the left and right parts of the building are coupled although the two parts are structurally isolated by the expansion joint. The 6 natural modes are composed of in-phase and out-of-phase vibrations in the x direction, y direction, and torsion. Table 1 is the summary of obtained modal properties before and after the retrofit. Obtained dynamic properties from BD2 excitation were almost identical to those from BD1 excitation, and thus were not shown in this paper.

3. Model updating based on RSM and MOO

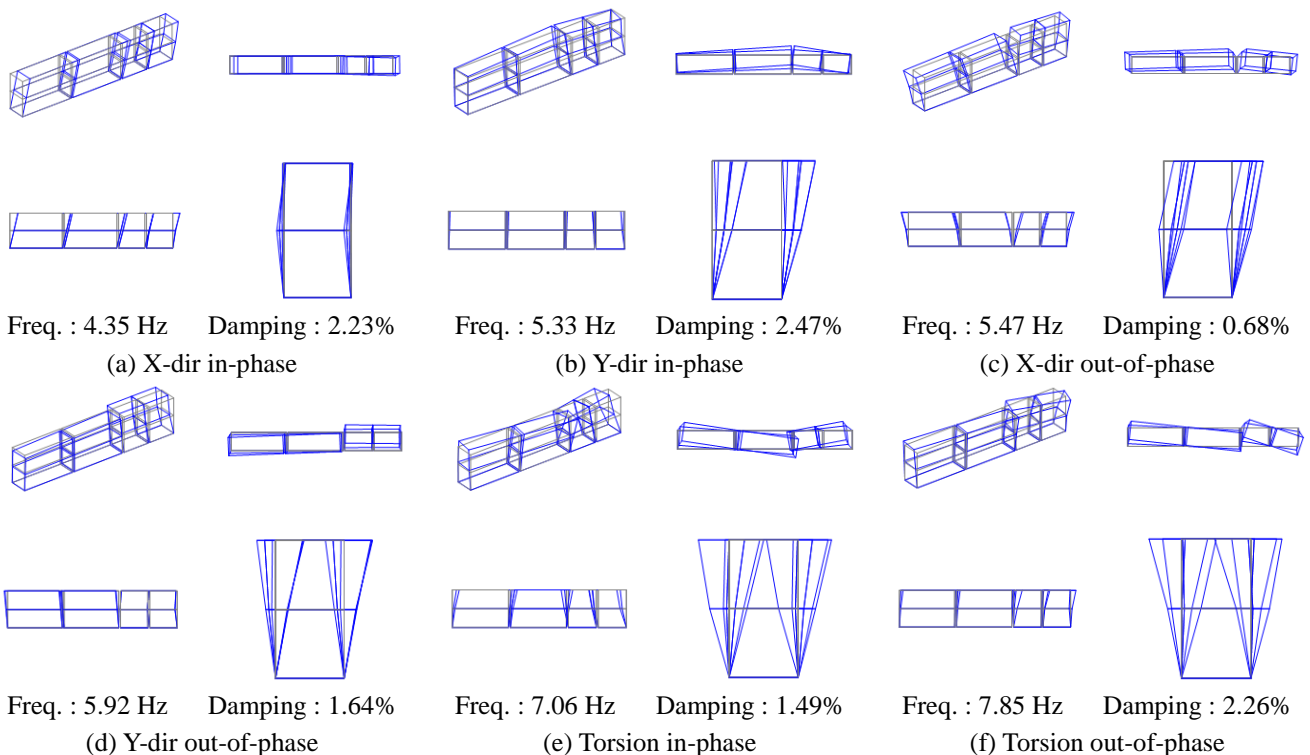


Fig. 4 Identified mode shapes (BD1 shaking, before retrofit)

The RS method is a statistical analysis method to obtain approximate multivariate functions describing the response surface. Generally, predicted relationships are expressed as a polynomial function with different orders. The most commonly used function in the RS method is the second-order polynomial, which can be expressed as

$$y = \beta_0 + \sum \beta_i x_i + \sum \beta_{ij} x_i x_j + \sum \beta_{ii} x_i^2 + \varepsilon, \quad (1)$$

where β is the undetermined regression coefficient; x is the design variable; and ε is the residual error.

The sampling points (i.e., parameter combinations) to obtain the second-order response surface can be determined using the Central Composite Design (CCD). The sampling points in CCD include the axis points and central points in addition to those of factorial design. Therefore, the number of samples necessary for a CCD design is $n = 2^k + 2k + n_c$, where k is the number of parameters and n_c is the number of center point samples set as 1 in this study. In the regression analysis, the significance of each term in Eq. (1) is examined using the analysis of variance (ANOVA) method, and the final function is determined after non-significant parameters are dropped out. A detailed procedure of the RS method using CCD can be found in the literature (Myers and Montgomery 2002).

After the FE analyses are performed using the parameter combinations determined by CCD, two types of residuals as shown in Eq. (2) and Eq. (3) were computed, which are the RMSE (Root mean square error) of the natural frequency residuals and the average error in mode shapes, i.e., the complement of the average of the MAC (Modal Assurance criterion) values, respectively.

$$e_1 = \sqrt{\frac{1}{N} \sum_{j=1}^N \left(\frac{f_{j,a} - f_{j,m}}{f_{j,m}} \right)^2} \quad (2)$$

$$e_2 = \frac{1}{N} \sum_{j=1}^N (1 - MAC_j) \quad (3)$$

where MAC_j denotes the MAC value of the j -th mode, defined as

$$MAC_j = \frac{\{\phi_{j,a}^T \phi_{j,m}\}^2}{\{\phi_{j,a}^T \phi_{j,a}\} \{\phi_{j,m}^T \phi_{j,m}\}} \quad (4)$$

Here, $f_{j,a}$ and $f_{j,m}$ represent the analytical and measured natural frequencies of the j -th mode; $\phi_{j,a}$ and $\phi_{j,m}$ the analytical and measured mode shapes of the j -th mode, respectively; and N indicates the number of modes used in the computation.

Subsequently, the RS method was employed to yield two RS functions corresponding to e_1 and e_2 , respectively. The accuracy of regression is generally quantified by the coefficients of determination, i.e., R^2 and R_{adj}^2 . Since a value of R^2 is automatically and spuriously increasing when additional parameters (even non-significant ones) are added to the model, an R_{adj}^2 that adjusts for the number of parameters in a model relative to

the number of data points is used as a supplementary evaluation. An RS model is well fitted with the samples if both R^2 and R_{adj}^2 are large. However, a well-fitted model does not always accurately predict the responses of the unseen values of input parameters. Hence as a third criterion, the normal regression parameter of PRESS, R_{pred}^2 , is also considered. The PRESS (predicted residual error sum of squares) is computed via the leave-one-out cross validation process by adding the square of the residuals when each sample is left out in turn, as represented in Eq. (5).

$$R_{pred}^2 = 1 - \frac{\sum_{i=1}^n (y^{(i)} - y_{pred}^{(i)})^2}{\sum_{i=1}^n (y^{(i)} - \bar{y})^2}, \quad (5)$$

where $y^{(i)}$ is the i -th measurement, $y_{pred}^{(i)}$ is the prediction of the model in which $y^{(i)}$ is left out, and \bar{y} is the mean of all measurements. R_{pred}^2 measures the capability of the model to predict future values and is more sensitive measure for the accuracy of the RS function.

Obtained RS functions are used as the objective functions for optimization. This study employed NSGA-II, which is a kind of the advanced algorithms in MOO. The accuracy of Pareto solutions would depend on the accuracy of the RS functions. If R_{pred}^2 is low, there exist large differences between the predicted response and the actual behavior. In practice, the accuracy of the RS model depends on the range of the parameters used in CCD. Therefore, iterative estimation of RS functions using adjusted CCD table (i.e., adjusted bounds) is required. In this study, adjustment of the CCD table is performed based on the parameter values of the Pareto solutions. That is, the upper and lower bounds are set as the maximum and the minimum of each parameter of the Pareto solutions, respectively. The central point for CCD is set as the average of the upper and lower bounds. However, when the accuracy of the RS function is not high enough, obtained Pareto solutions can be located far from the optimal point. In this case, extended bounds from the range of the Pareto solutions is appropriate.

Once the Pareto-optimal set is found from an RS model with sufficiently high R_{pred}^2 values, the next task is to choose one of them as the final solution. Since all of the Pareto solutions are considered equally good in MOO, a decision on the final solution among the Pareto solutions requires additional information or experts' preferences. The final solution may be determined as one of the Pareto solutions that have the minimum in the sum of the errors in objective functions. However, when the errors have different scales, the results would be biased.

In this paper, the TOPSIS procedure is used to find the best compromise solution. The concept of TOPSIS is that the preferred solution should not only have the shortest distance from the positive ideal solution, but also have the longest distance from the negative ideal solution (Huang 2011, Behzadian *et al.* 2012).

The overall procedure for model updating in this study can be summarized as Fig. 5.

4. FE modeling and updating

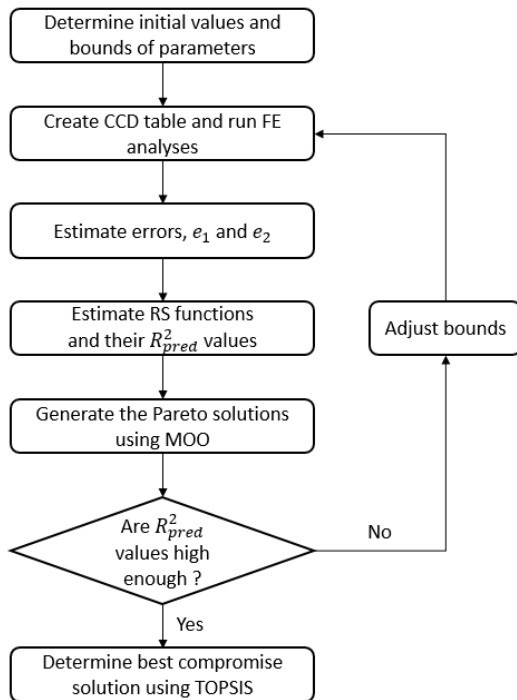


Fig. 5 Procedure of model updating

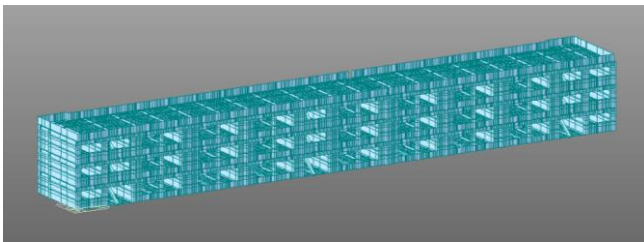


Fig. 6 FE modeling of the test building using commercial software

4.1 Initial model and updating of FE model (before retrofit)

The initial FE model of the test building is constructed using the proprietary FE analysis program Midas Gen (2004), as shown in Fig. 6, based on the information provided in structural drawings, as well as data obtained from the detailed field inspection. Conventional assumptions for modeling of building structures (lumped mass and rigid diaphragm) were used.

The elastic modulus of concrete (E_c), elastic modulus of masonry (E_m), and stiffness of the elastic links in the normal direction (k_x) and in the tangential direction (k_y) were selected as the updating parameters. The elastic modulus of concrete was evaluated using Eq. (6) provided in the Korean Building Code (2016) from the concrete strength obtained from the Schmidt hammer test.

$$E_c = 8500 \sqrt[3]{f'_c}, \quad (\text{MPa}) \quad (6)$$

where f'_c is the compressive strength of the concrete. It was reported in ACI 318 (2011) that the actual modulus of the concrete can be varied about 20% from the specified value in Eq. (6). Thus, the range of 0.8-1.2 was used as the

Table 2 Bounds for the first CCD

Coded value	Lower bound	Central point	Upper bound
	-0.5	0	0.5
E_c (MPa)	24488.1	27209.0	29929.9
E_m (MPa)	1422.0	1706.5	1990.9
k_x (N/mm)	18506.8	28518.5	18911.3
k_y (N/mm)	8191.8	13551.5	18911.3

Table 3 Parameters for NSGA-II

Parameters	Values
Population Size	50
Number of iterations	200
Crossover probability	0.90
Mutation probability	1/n
Crossover index	5
Mutation index	20

bound for this parameter in CCD.

The masonry infills were included in the FE model using the shell elements. The masonry infills have a thickness of 190 mm. The elastic modulus of masonry infills was assumed to be between 1138 MPa and 2275.3 MPa according to ASCE 41-06 (2007), which correspond to the values when the masonry condition is poor and fair, respectively.

As observed in identified mode shapes, the behaviors of the left and right parts of the building are coupled. Thus, in the FE model, two parts were connected using elastic link elements at the expansion joint. The expansion joints were filled with asphalt caulking according to architectural drawings. The spring constants of the elastic links were determined using the material properties of asphalt caulking ($E=0.7-4.0$ MPa and $G=E/3-E/2$) and the contacting area of the expansion joint. The resulting range of the spring constants was computed as 8495-48542 N/mm in the normal direction and 2832-24271 N/mm in the tangential direction.

The model updating procedure based on the RS method and the MOO stated previously were performed subsequently. The combination of parameters for FE analyses was generated according to the CCD. Table 2 shows the bounds for the CCD table.

Estimation of the RS functions and subsequent optimization was performed. Using the NSGA-II with the parameters of Table 3, a total of 18 Pareto solutions were obtained. The R_{pred}^2 values for the first RS functions are shown in Table 4. J_1 and J_2 in Table 4 denote obtained RS functions from e_1 and e_2 , respectively, through the multivariate regression. Since the R_{pred}^2 value for J_2 of the initial RS model is quite low, it is expected that the prediction of the mode shapes is somewhat inaccurate. Thus, the obtained Pareto solutions were not considered as candidates for the final solution. Instead, iterative estimation via CCD using modified bounds and a new RS model was performed. As mentioned previously, since the R_{pred}^2 was quite low, modified bounds were extended and set as 90% of the minimum values and 110% of the

Table 4 R^2 values of the RS models (before retrofit)

	1st RS model		2nd RS model	
	J_1	J_2	J_1	J_2
R^2	0.999	0.733	1.000	0.991
R_{adj}^2	0.999	0.662	1.000	0.986
R_{pred}^2	0.964	0.155	0.929	0.971

Table 5 Updated parameter (before retrofit)

Parameters	Initial guess	Updated value	Changes (%)
E_c (MPa)	27209	28531	5%
E_m (MPa)	1706.45	2245	32%
k_x (N/mm)	28518.5	42382	49%
k_y (N/mm)	13551.5	19104	41%

Table 6 Natural frequencies and MAC values (before retrofit)

Mode	Natural Frequencies			MAC
	Measured (Hz)	Initial model (Hz)	Updated model (Hz)	Updated model (Hz)
1st	4.35	3.87 (-11.0%)	4.24 (-2.6%)	0.96
2nd	5.33	4.87 (-8.5%)	5.48 (2.9%)	0.64
3rd	5.47	5.03 (-8.1%)	5.63 (3.0%)	0.84
4th	5.92	5.57 (-6.0%)	6.18 (4.4%)	0.91
5th	7.06	6.13 (-13.1%)	6.84 (-3.1%)	0.92
6th	7.85	6.74 (-14.1%)	7.61 (-3.1%)	0.96

maximum values of the obtained Pareto solutions. Subsequent MOO using new RS functions also yielded 18 Pareto solutions. Since the R_{pred}^2 values at the second RS functions were sufficiently high as shown in Table 4, no further iterations were performed and the final solution was found among the Pareto solutions. Fig. 7 shows bounds for CCD and the changes in the parameter values of the Pareto solutions with iteration.

The final solution was determined using the TOPSIS procedure, which identifies a compromise set that has the shortest distance from the ideal solution and the longest distance from the worst solution. This concept is useful when the criteria for selection have different scaling and variation ranges. For example, one can choose a final solution that has the minimum of the weighted sum of the errors (the RMSE of natural frequencies and errors in mode shape in this study), but it is unclear if chosen weighting factor is optimal. The TOPSIS procedure provides an objective weighting considering the variation of errors rather than subjective judgement.

In this study, 12 error terms (composed of the natural frequency errors and mode shape errors in the 1st to 6th mode) were evaluated from FE analysis using the parameter set of the final Pareto solutions, which were then used for the decision matrix for the TOPSIS. For the purpose of illustration, obtained best compromise solution is indicated on e_1 and e_2 space in Fig. 8. Also the values of the solution are indicated in Fig. 7 with arrows.

Parameters of the best compromise solution and changes from the initial guess are shown in Table 5, and the dynamic properties of the final updated model were compared with

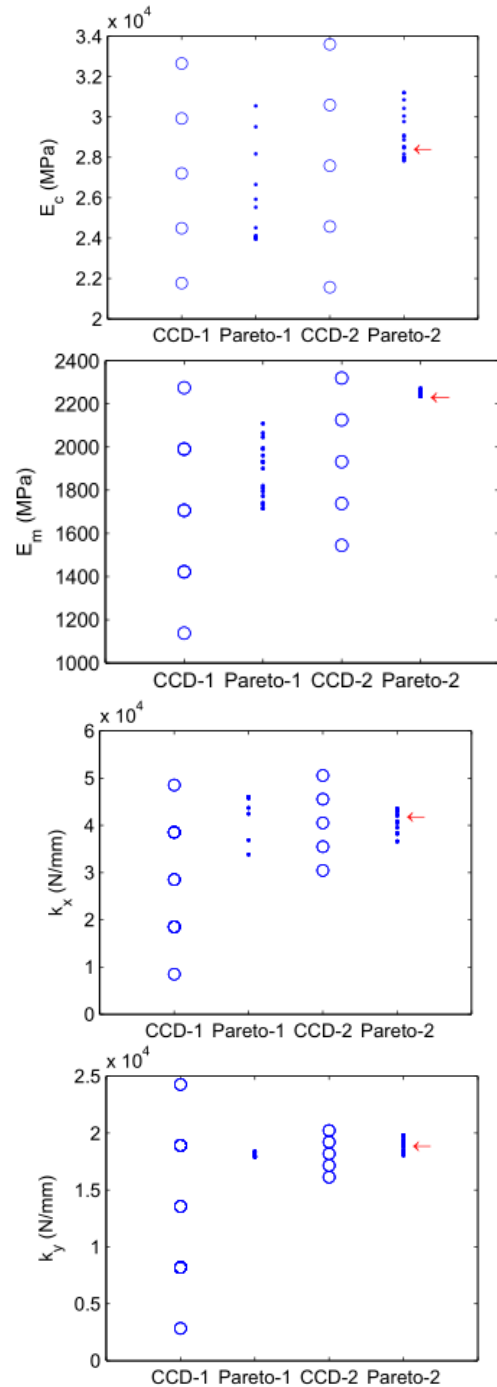


Fig. 7 Distribution of parameters with iteration (before retrofit)

the measured ones, shown in Table 6.

4.2 Updating of FE model (after retrofit)

The FE model for the building after retrofit was constructed by reflecting the modifications made during the retrofit. The elastic modulus of existing concrete and masonry walls were kept unchanged from the updated model for pre-retrofit. The updating parameters for the model after retrofit were selected as the elastic modulus of concrete of the new shear wall (E_c), effective stiffness

Table 7 Bounds for parameters (after retrofit)

	Bounds			
	E_c of shearwall (MPa)	α	k_x (N/mm)	k_y (N/mm)
1st CCD	1349-26986	5%-100%	42382-127145	19104-57312
2nd CCD	2674-3261	16%-24%	113623-138889	34967-56570

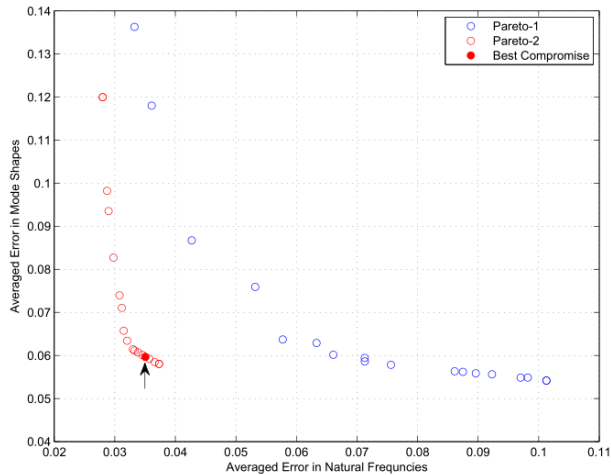


Fig. 8 Pareto solutions and best compromise solution (before retrofit)

 Table 8 R^2 values of the RS models (after retrofit)

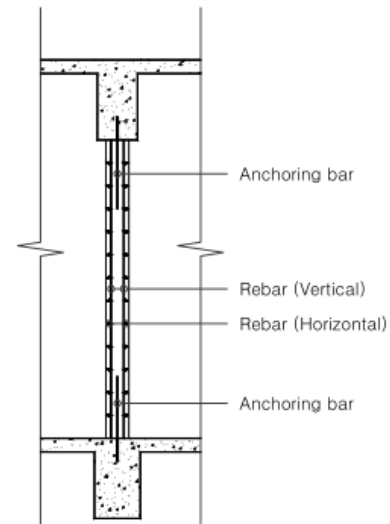
	1st RS model		2nd RS model	
	J_1	J_2	J_1	J_2
R^2	0.689	0.993	0.998	0.997
R^2_{adj}	0.650	0.991	0.995	0.995
R^2_{pred}	0.194	0.969	0.954	0.974

factor for jacketed members (α), and spring constants of the elastic link at the expansion joint (k_x and k_y).

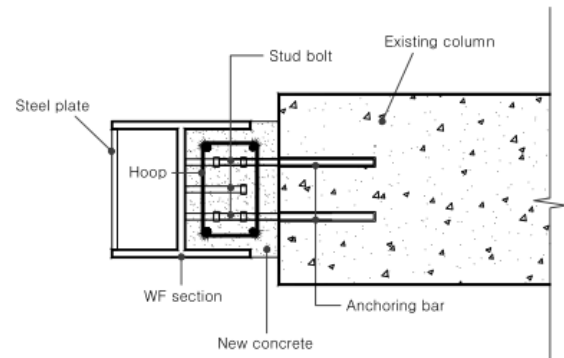
The bounds for parameters are shown in Table 7. The bound for the effective stiffness factor of the jacketed members was set as 0.05-1.0 since the stiffness of the jacketed members was considered to be lower than that of fully composite section. The bounds for E_c of new shear wall concrete followed a similar assumption because added shear walls were not continuous vertically, even though even though they are connected to bottom of the beams and top of floor slabs using anchoring rebars (Fig. 9). In the case of elastic link stiffness, the stiffness was expected to increase since the details of expansion joints were repaired. The upper bound of 3 times the updated values was set by engineering judgement.

Updating the FE model was performed using the same procedure as for the pre-retrofit. Identical objective functions were used for updating. As the case of pre-retrofit model, one iteration was required to obtain the final solution. Tables 7 and 8 show the bounds of the parameters and R^2_{pred} values per iteration.

Fig. 10 shows the Pareto solutions at the second analysis and the best compromise solution from TOPSIS. Updated parameters and resulting dynamic properties for retrofitted



(a) new shear wall



(b) steel wide section jacketing

Fig. 9 Details of added members

Table 9 Updated parameter (after retrofit)

Parameters	Initial guess	Updated value	Note
E_c of new concrete	26986 MPa	3160.1 MPa	12% of value using Eq. (6)
α	1.0	0.230	22% of fully composite section
k_x	127145N/mm	130217 N/mm	307% increase from pre-retrofit
k_y	57312N/mm	40081.9 N/mm	210% increase from pre-retrofit

Table 10. Natural frequencies and MAC values (after retrofit)

Mode	Natural Frequencies			MAC	
	Measured (Hz)	Initial model (Hz)	Updated model (Hz)	Initial model (Hz)	Updated model
1st	4.05	4.12 (-2.4%)	4.22 (-4.0%)	0.99	0.99
2nd	5.56	5.42 (-5.0%)	5.71 (-2.7%)	0.40	0.97
3rd	6.13	5.61 (-9.8%)	6.22 (-1.4%)	0.24	0.92
4th	6.76	6.14 (-9.2%)	6.76 (0.03%)	0.02	0.95
5th	7.23	6.73 (-6.3%)	7.18 (0.67%)	0.54	0.95
6th	8.46	7.50 (-10.5%)	8.38 (0.90%)	0.66	0.82

building are summarized in Table 9 and Table 10, respectively.

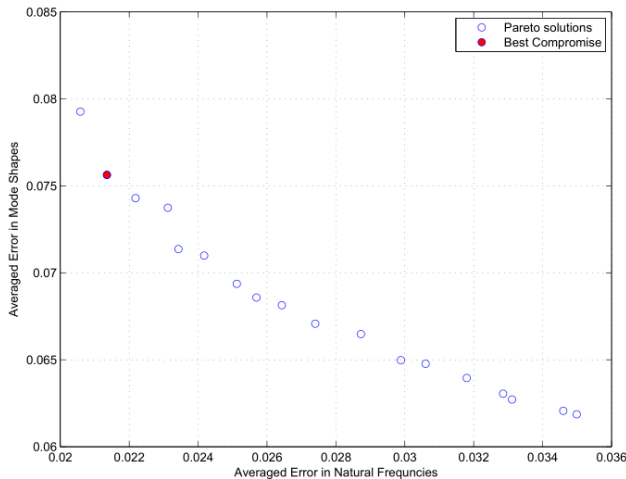


Fig. 10 Pareto solutions at the second iteration and best compromise solution (after retrofit)

Changes in the parameters from the initial guess before and after retrofit are shown in Table 5 and Table 9, respectively. In the case of building before retrofit, the elastic modulus of existing concrete has changed by 5% from the code proposed value, which seems reasonable considering small vibration amplitude during the test. The stiffness of the masonry also seems reasonable since the identified value is similar to ASCE 41-06 (2007) when the masonry condition is fair. However, the identified stiffness of jacketed members and added shear walls were much smaller than those for fully composite or monolithic sections. This might be caused by the condition of the interface between the new and existing concrete, which is completely different from the monolithically casted members. To identify the influence of such low stiffness of retrofitted and added members on the overall behavior, further research is needed, including the behavior in the nonlinear load range through the analytical and experimental investigations.

5. Conclusions

In this study, the FE model updating procedure based on the RS method and a Pareto-based MOO was formulated and applied for updating of a low-rise reinforced concrete building before and after the seismic retrofit. Vibration tests were performed to identify the modal properties of the building before and after the seismic retrofit. From identified mode shapes, coupled motion between two parts of the building separated by the expansion joint was observed and reflected in the FE model.

For updating of pre-retrofit building, the elastic modulus of concrete and masonry, and spring constants for the expansion joint were selected as the updating parameters. Two RS functions representing the errors in the natural frequencies and mode shape, respectively, were obtained and used as the objective functions for MOO. The best compromise solution was determined among the Pareto solutions using the TOPSIS procedure. A similar task was performed for the building after the retrofit by taking the

updating parameters as the stiffness of modified or added members.

Obtained parameters of the existing building were reasonably comparable with the current code provision. However, the stiffness of added concrete shear walls and steel section jacketed members was considerably lower than expectation. Such low values are seemingly because the bond between new and existing concrete is not as good as the monolithically casted members, even though they are connected by the anchoring bars.

Implications of identified parameters to overall performance of the structure needs to be further investigated and verified analytically and experimentally, including the behavior in the nonlinear range. Aside from the identified parameters, the model updating procedure proposed in this paper provides an efficient guideline for calibration of FE models using general-purpose analysis software.

References

- ACI (2011), Building Code Requirements for Structural Concrete, 318-11.
- Architectural Institute of Korea (2016), Korea Building Code, Ministry of Land, Transport and Maritime Affairs.
- ASCE/SEI (2007), Seismic Rehabilitation of Existing Buildings, ASCE/SEI 41-06, Reston.
- Behzadian, M., Otahgsara, S.K., Yazdani, M. and Ignatius, J. (2012), "A state-of-the-art survey of TOPSIS applications", *Exp. Syst. Appl.*, **39**(17), 13051-13069.
- Deb, K., Pratap, A., Agarwal, S. and Meyarivan, T.A.M.T. (2002), "A fast and elitist multiobjective genetic algorithm: NSGA-II", *IEEE Tran. Evol. Comput.*, **6**(2), 182-197.
- Deng, L. and Cai, C.S. (2009), "Bridge model updating using response surface method and genetic algorithm", *J. Bridge Eng.*, **15**(5), 553-564.
- Fang, S.E. and Perera, R. (2009), "A response surface methodology based damage identification technique", *Smart Mater. Struct.*, **18**(6), 065009.
- Fang, S.E. and Perera, R. (2011), "Damage identification by response surface based model updating using D-optimal design", *Mech. Syst. Signal Pr.*, **25**(2), 717-733.
- Fang, S.E., Perera, R. and De Roeck, G. (2008), "Damage identification of a reinforced concrete frame by finite element model updating using damage parameterization", *J. Sound Vib.*, **313**(3), 544-559.
- Friswell, M. and Mottershead, J.E. (1995), *Finite Element Model Updating in Structural Dynamics*, Springer Science.
- Huang, J.J. and Yoon, K. (2011), *Multiple Attribute Decision Making: Methods and Applications*, Chapman and Hall.
- Jaishi, B. and Ren, W.X. (2006), "Damage detection by finite element model updating using modal flexibility residual", *J. Sound Vib.*, **290**(1), 369-387.
- MIDAS IT (2004), MIDAS/GEN Version 6.3. 2 User's Manual.
- Montgomery, D.C. (2008), *Design and Analysis of Experiments*, John Wiley & Sons.
- Myers, R.H. and Montgomery, D.C. (2002), *Response Surface Methodology: Process and Product Optimization Using Designed Experiments*, 2nd Edition, Wiley
- Ren, W.X. and Chen, H.B. (2010), "Finite element model updating in structural dynamics by using the response surface method", *Eng. Struct.*, **32**(8), 2455-2465.
- Shahidi, S.G. and Pakzad, S.N. (2013), "Generalized response surface model updating using time domain data", *J. Struct. Eng.*, **140**(8), A4014001.

- Teughels, A., Maeck, J. and De Roeck, G. (2002), "Damage assessment by FE model updating using damage functions", *Comput. Struct.*, **80**(25), 1869-1879.
- Van Overschee, P. and De Moor, B. (1993), "N4SID: numerical algorithms for state space subspace system identification", *Proceedings of the World Congress of the International Federation of Automatic Control*.
- Yu, E. and Chung, L. (2012), "Seismic damage detection of a reinforced concrete structure by finite element model updating", *Smart Struct. Syst.*, **9**(3), 253-271.
- Yu, E., Taciroglu, E. and Wallace, J.W. (2007), "Parameter identification of framed structures using an improved finite element model-updating method-Part I: formulation and verification", *Earthq. Eng. Struct. Dyn.*, **36**(5), 619-639.
- Zitzler, E. and Thiele, L. (1999), "Multiobjective evolutionary algorithms: a comparative case study and the strength Pareto approach", *IEEE Tran. Evol. Comput.*, **3**(4), 257-271.

CC